Laser and Particle Beams (2002), *20*, 109–112. Printed in the USA.

DOI: 10.1017.S0263034602201159

Energy spectra of Ag, Au, Sn, and Pb ions emitted from laser-created plasmas determined from their implantation depth profile in a metallic substrate

JOSEF KRÁSA,[1] LEOŠ LÁSKA,[1] KAREL ROHLENA,[1] VRATISLAV PEŘINA,[2] AND VLADIMÍR HNATOWICZ[2]

[1]Institute of Physics ASCR, Na Slovance 2, 182 21 Prague 8, Czech Republic
[2]Nuclear Physics Institute ASCR, 250 68 Řež, Czech Republic

(Received 29 January 2001; Accepted 14 November 2001)

Abstract

The energy spectra of heavy ions emitted from laser-produced plasmas were determined by the use of a technique relying on the implantation of plasma ions into a substrate located close to the plasma. Ion energy spectra were reconstructed from depth profiles of the implanted ions measured by the standard Rutherford back-scattering (RBS) technique employing 2 MeV alpha particles scattered at 170° laboratory angle. The energy spectra of Ag, Au, Sn, and Pb ions, implanted into aluminum or steel foils, are presented. A review of other techniques for ion energy spectrum measurement is presented and their limitations are discussed.

Keywords: Ion energy distribution; Ion implantation; Laser-produced plasma

1. INTRODUCTION

Measurement of energy distribution of ions emitted from laser-generated plasma is based on use of an electrostatic ion energy analyzer (EIA) and of a Thomson parabola spectrometer (TPS; Láska *et al.*, 1996*a*; Woryna *et al.*, 1996; Clark *et al.*, 1999; Mróz *et al.*, 2000). The velocity spectrum is usually evaluated from a charge-integrated and time-resolved current detected with an ion collector (IC; Zacharenkov *et al.*, 1983). All the methods need calibrated ion detectors to determine number of ions carrying a charge q and moving with velocity v_i or with kinetic energy E_i. An EIA is commonly equipped with an open electron multiplier (EM) for its very high electron gain. Its disadvantage consists in the dependence of its gain on the energy and charge state of ions as well as on the impact position of ions on the first dynode surface (Krása *et al.*, 1999). Ions with lower energy passing through $\underline{E} \parallel \underline{B}$ fields of a TPS are usually detected with a microchannel plate (MCP), the gain of which depends on properties of the detected ions, too (Stockli & Fry, 1997). Only very fast ions can be detected with a track detector CR39 employed instead of a MCP(Clark *et al.*, 1999). The etched pits on the CR39 surface can be counted and an ion spectrum may be determined from the energy dispersion along the parabola. Nowadays, MCPs, EMs, and other ion detectors have been calibrated with well-defined ion beams produced by ion sources like EBIS, CRYEBIS, and so on (Stockli & Fry, 1997; Krása *et al.*, 1999; Mróz *et al.*, 2000).

There is no universal technique able to measure the energy distribution over the full range of energy, E, as well as charge state, q, of emitted ions. As was mentioned above, the use of a TPS is limited by sensitivity and by dynamic range of an employed ion detector. The track detector can give the absolute number of ions hitting its surface with kinetic energy higher than 100 keV/nucleon. Very sensitive multichannel plates show nonlinear response to all parameters of impacting ions. Their calibration is a complex procedure and should also include a calibration of the optical system that makes the computer reading of MCP response possible. This technique should enable the determination of $dN(q,E)/dE$ to be done for a single laser shot. On the contrary, the determination of $dN(q,E)/dE$ by use of EIA needs many laser shots of the same quality because the EIA must be retuned for a large set of values of ion energy per charge state, E/q, to measure over the whole range of E as well as of q. If a calibrated EM is used for detection of ions, the total energy spectrum is a sum of partial distributions $dN(q,E)/dE = \Sigma_q(dN_q/dE)$. Nevertheless, the use of EIA makes the

Address correspondence and reprint requests to: J. Krása, Institute of Physics, ASCR, Na Slovance 2, 182 21 Prague 8, Czech Republic. E-mail: krasa@fzu.cz

estimation of both the charge-state range and ion-energy range possible (Laska *et al.*, 1996*b*).

2. PRINCIPLES OF METHOD

A new technique for measurement of total ion energy distribution $dN(q,E)/dE = \Sigma_q(dN_q/dE)$ was based on an absorption technique relying on the implantation of plasma ions into a light element target located close to the laser-produced plasma. Ion energy spectra can be reconstructed from the depth profile of implanted ions measured by some common depth profiling techniques such as RBS or SIMS. In the measurement presented, Al and steel substrates were analyzed by the standard Rutherford back-scattering technique applying 2 MeV alpha particles scattered at 170° laboratory scattering angle (Peřina *et al.*, 1998). The alpha particles are back scattered with different energies depending on the kind of scattering species as Figure 1 shows. It is evident that the resolution of scattering elements by energy of back-scattered alpha particles is very high if heavy ions are implanted into a light material. The signal from alpha particles scattered on Al substrate in a low energy region up to the edge of 1200 keV dominates. The peak at 1870 keV corresponds to the scattering on surface silver atoms. The scattering of alpha particles on the Ag atoms incorporated at different depths under the Al foil surface is registered on the left-hand side of the Ag peak by a long tail. From this part of the RBS spectrum, the depth profile of the amount of implanted ions can be determined employing a customary procedure (Saarilahti & Rauhala, 1992; Tesmer & Nastasi, 1995). Figure 1 shows an example of the RBS spectrum, plot (A), and the depth profile, plot (B), of Ag in Al foil, calculated by GISA3 code (Saarilahti & Rauhala, 1992). The energy of alpha particles was transformed into the depth applying stopping powers calculated with the RSTOP subroutine adopted from TRIM (version 91) code (Saarilahti & Rauhala, 1992; Ziegler *et al.*, 1995). The depth can be converted into the initial energy of implanted ions by use of the PRAL code (Biersack, 1982). This analytical code gives the projected range and the range straggling of implanted ions as functions of the initial energy of ions for any ion–target combination. The density of the incorporated ions at a given depth gives relative fluence of the ions with given initial energy.

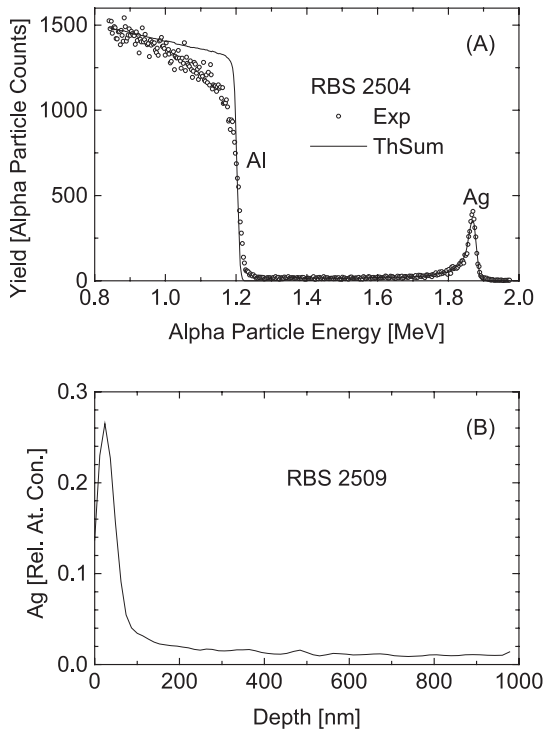

Fig. 1. The RBS spectrum measured on the Al sample implanted with Ag ions (A). The depth profile of Ag atoms under the Al foil surface (B). The Al foil was located near the target normal ($E_{2\omega} \approx 12$ J, $I_L \approx 1 \times 10^{14}$ W/cm^2).

3. EXPERIMENTAL SETUP

The iodine laser system PERUN operating at the fundamental wavelength ($\lambda = 1315$ nm) as well as at the second harmonics ($\lambda = 657$ nm) was used as a driver (Láska *et al.*, 1996*a*). The available energy of 350-ps laser pulses was 45 J. The maximum power density delivered on a target was slightly above 1×10^{15} W/cm^2. The minimum diameter of the focal spot was about 100 μm.

The ion emission from the laser-produced plasma was measured with collectors, a cylindrical electrostatic ion analyzer, and a Thomson parabola spectrograph (Láska *et al.*, 1996*a*; Krása *et al.*, 1998). Drift lengths were 83–187 cm for ICs, and around 210 cm for IEA and TPS. The schematic diagram of experimental arrangement is shown in Figure 2. The distance of the implanted samples S1 and S2 from the irradiated target was usually less then 10 cm. From 10 to 30 laser pulses were applied in each experiment in order to accumulate a measurable amount of ions implanted into different samples.

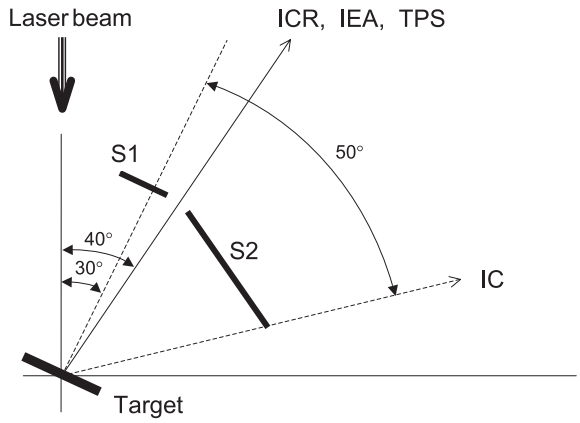

Fig. 2. Schematic diagram of experimental arrangement. IC and ICR: ion collectors; IEA: ion energy analyzer; TPS: Thomson parabola spectrograph; S1 and S2: foils bombarded by ions escaping from the laser-produced plasma on the target.

https://doi.org/10.1017/S0263034602201159 Published online by Cambridge University Press

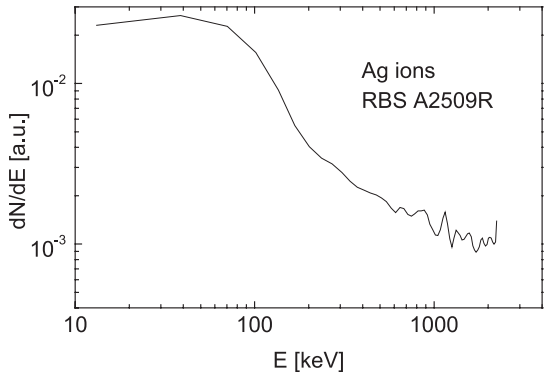

Fig. 3. Energy distribution of Ag ions emitted from a plasma generated by power density of about 1×10^{14} W/cm^2 and implanted into the Al substrate. The distribution was derived from the RBS spectrum; see Figure 1.

4. RESULTS

Ion energy spectra determined from depth profiles of different ions implanted into thick substrates are shown in Figures 3–7 for ion energies higher then 10 keV. This value is a low energy limit of the used experimental technique. Figure 3 shows the energy distribution of Ag ions emitted from plasma produced by laser pulses of average energy of 12 J ($I_L \approx 1 \times 10^{14}$ W/cm^2). The confirmation of slow and fast ion groups generation by the laser–target interaction can be found on the E-axis at about 200 keV because the slowing down of the decrease in dN/dE is evident. The high-energy ion group is detectable up to ≈2 MeV. The noisy shape of the spectrum around 1 MeV corresponds to the stopping power of Ag ions in the Al substrate and to the interference of the Ag signal with the signal from the Al substrate below the Al edge at 1.2 MeV (see Fig. 1A). The relatively large portion of high-energy ions can be explained due to the fact that by this technique all ions are registered with proper energy regardless of their charge state or of possible recombination on the way to the substrate.

The energy spectrum of Au ions produced by the second harmonics ($E_L \approx 28$ J, $I_L \approx 5 \times 10^{14}$ W/cm^2) of the iodine laser is shown in Figure 4. The highest energy of Au ions determined from the maximum depth of implantation into Al is 2 MeV. The corresponding depth of Au implantation into Al substrate was about 460 nm. One can compare this energy spectrum with Au ion charge state–ion energy distribution shown in Figure 5 that was measured under similar experimental conditions with use of IEA (Láska *et al.*, 2000*a*). This measurement presents the upper range of ion energy of about 7 MeV while the implantation technique gives only a 2-MeV upper limit. It may be due to the higher sensitivity of IEA given by the negligible "dark" current of the EM and the starting interference of the RBS signal at ≈1 MeV mentioned above. Two ion groups emitted from the Au plasma can be distinguished in Figure 5. The slow group dominates in the energy range up to about 250 keV, as labeled by the arrow, and the fast group consists of ions with energy up to 7 MeV. Nearly at the same value of energy, the critical point, from which the slowing down in the decrease in dN/dE starts, can be found in Figure 4.

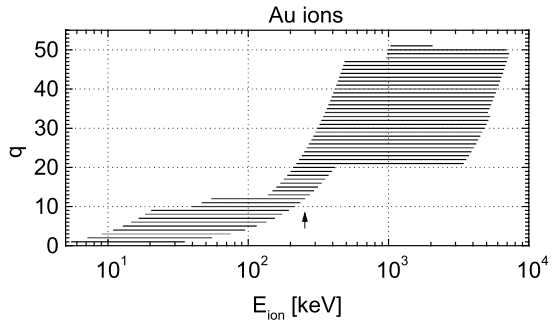

Fig. 5. Charge state–kinetic energy distribution of ions emitted from plasma created by a 27-J laser pulse focused on an Au target and measured with a cylindrical electrostatic ion energy analyzer (Láska *et al.*, 2000*b*).

The ions of Pb plasma, generated by the fundamental laser frequency ($E_L \approx 22$ J, $I_L \approx 5 \times 10^{14}$ W/cm^2) of the iodine laser, were implanted into a Ck-45 steel substrate to modify the surface properties of the steel (Láska *et al.*, 2000*a*). The maximum depth of implantation was about 250 nm. The corresponding maximum ion energy is about

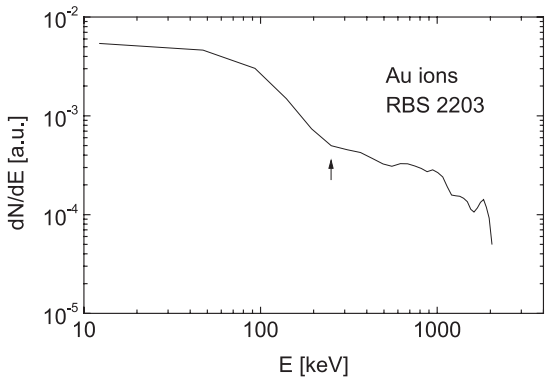

Fig. 4. Energy distribution of Au ions emitted from laser-produced plasma ($I_L \approx 5 \times 10^{14}$ W/cm^2) and determined from the depth profile of Ag concentration incorporated into the Al substrate.

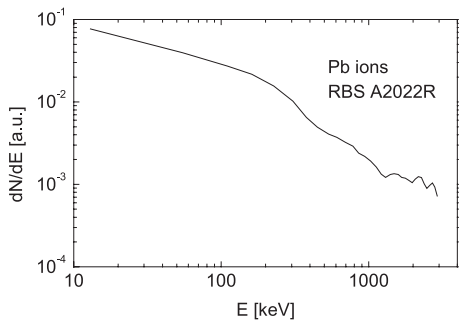

Fig. 6. Energy distribution of Pb ions determined from a RBS spectrum measured on a steel sample implanted with Pb ions emitted from a laser-produced plasma ($E_L \approx 22$ J, $I_L \approx 5 \times 10^{14}$ W/cm^2).

https://doi.org/10.1017/S0263034602201159 Published online by Cambridge University Press

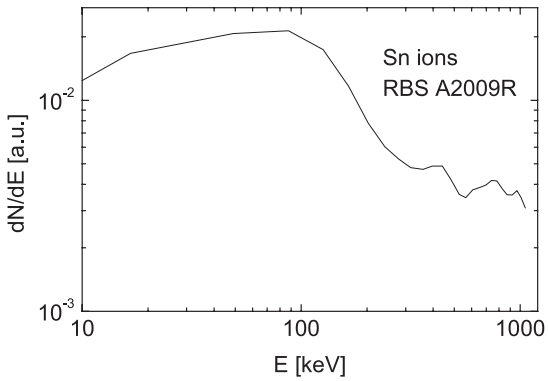

Fig. 7. Energy distribution of Sn ions determined from a RBS spectrum measured on a steel sample implanted with Sn ions emitted from a laser-produced plasma ($E_L \approx 22$ J, $I_L \approx 5 \times 10^{14}$ W/cm^2).

3 MeV as Figure 6 shows. The number of detected Pb atoms decreased from 1.4×10^{16} cm^{-2} near the surface to 6.5×10^{14} cm^{-2}. The energy separating the fast ion group from the slow one is about 400 keV. It is possible to assume that the slow group consists of ions carrying a charge state up to ≈15+ and the fastest ions have a charge state of ≈50+ as it was presented in (Kráska *et al.*, 1998*a*) for similar experimental conditions.

Figure 7 shows the energy distribution of Sn ions generated by the fundamental laser frequency ($E_L \approx 22$ J, $I_L \approx 5 \times 10^{14}$ W/cm^2) of the iodine laser. Sn ions were implanted also into a Ck-45 steel substrate to modify the surface properties of the steel to reduce the friction coefficient (Láska *et al.*, 2000*a*). The number of Sn atoms near the surface is 4.9×10^{15} cm^{-2} and 0.65×10^{15} cm^{-2} in the depth of 175 nm corresponding to the impact energy of about 4 MeV. The group of fast ions dominates over the range starting from ≈250 keV.

5. CONCLUSION

The presented method for determination of the initial energy distribution of particles implanted into a substrate opens the way to determination of the ion energy distribution up to 5 MeV with the energy resolution of 10–20% for higher ion energy (>200 keV). The main advantage of this technique is the possibility of operating with extremely high ion fluxes. Thanks to this, the ion energy distributions can be measured at a distance of several centimeters from a target irradiated with a focused high power laser beam.

ACKNOWLEDGMENTS

This work was supported by the grant A1010819 from the Grant Agency of the Academy of Sciences of the Czech Republic.

REFERENCES

Biersack, J.P. (1982). New projected range algorithm as derived from transport equations. *Z. Phys. A* **305**, 95–101.

Clark, E.L., Krushelnick, K., Zepf, M., Tatarakis, M., Beg, F.N., Santala, M.I.K., Watts, I., Dangor, A.E., Norreys, P.A. & Machacek, A. (1999). Multi MeV heavy ion emission from ultra-intense laser-plasma interactions. RAL Report No. RAL-TR-1999-062, pp. 29–30.

Krása, J., Láska, L., Mašek, K., Pfeifer, M., Králiková, B., Skála, J., Straka, P., Rohlena, K., Mróz, W., Woryna, E., Parys, P., Wolowski, J., Haseroth, H., Golubev, A.A. & Sharkov, B.Yu. (1998). Multiply charged ions from iodine laser-produced plasma of medium- and high-Z targets. *Laser Part. Beams* **16**, 5–12.

Krása, J., Pfeifer, M., Stöckli, M.P., Lehnert, U. & Fry, D. (1999). The effect of the first dynode's geometry on the detection efficiency of a 119EM electron multiplier used as a highly charged ion detector. *NIM B* **152**, 397–402.

Láska, L., Juha, L., Krása, J., Mašek, K., Pfeifer, M., Rohlena, K., Králiková, B., Skála, J., Peřina, V., Hnatowicz, V., Woryna, E., Wolowski, J., Parys, P., Boody, F.P., Höpfl, R. & Hora, H. (2000*a*). Laser induced direct implantation of ions. *Czech. J. Phys.* **50**, Suppl. 3, 81–90.

Láska, L., Krása, J., Mašek, K., Pfeifer, M., Králiková, B., Mocek, T., Skála, J., Straka, P., Trenda, P. & Rohlena, K. (1996*a*). Iodine laser production of highly charged Ta ions. *Czech. J. Phys.* **46**, 1099.

Láska, L., Krása, J., Mašek, K., Pfeifer, M., Rohlena, K., Králiková, B., Skála, J., Woryna, E., Parys, P., Wolowski, J., Mróz, W., Sharkov, B. & Haseroth, H. (2000*b*). Properties of iodine laser-produced stream of multiply charged heavy ions of different elements. *Rev. Sci. Instrum.* **71**, 927–930.

Láska, L., Krása, J., Mašek, K., Pfeifer, M., Trenda, P., Králiková, B., Skála, J., Rohlena, K., Woryna, E., Farny, J., Wołowski, J., Mróz, W., Shumshurov, A., Sharkov, B., Collier, J., Langbein, K. & Haseroth, H. (1996*b*). Multiply charged ion generation from NIR and visible laser-produced plasma. *Rev. Sci. Instrum.* **67** 950–952.

Mróz, W., Norek, P., Prokopiuk, A., Parys, P., Pfeifer, M., Láska, L., Stöckli, M.P., Fry, D. & Kasuya, K. (2000). Method of processing ion energy distributions using a Thomson parabola ion spectrograph with a microchannelplate image converter camera. *Rev. Sci. Instrum.* **71**, 1417–1420.

Peřina, V., Hnatowicz, V., Krása, J. & Láska, L. (1998). Simple technique for measurement of energy spectra of ions from laser produced plasma. *Czech. J. Phys.* **48**, 1067–1073.

Saarilahti, J. & Rauhala, E. (1992). Interactive PC data analysis of ion backscattering spectra. *NIM B* **64**, 734–738.

Stockli, M.P. & Fry, D. (1997). Analog particle gain of microchannel plates for 1.5–154 keV/q Ar^{q+} ($3 \leq q \leq 16$). *Rev. Sci. Instrum.* **68**, 3053–3060.

Tesmer, J.R. & Nastasi, M., Eds. (1995). *Handbook of Modern Ion Beam Materials Analysis*, Vol. 1. Pittsburgh: Material Research Society.

Woryna, E., Parys, P., Wołowski, J. & Mróz, W. (1996). Corpuscular diagnostics and processing methods applied in investigation of laser-produced plasma as a source of highly ionized ions. *Laser Part. Beams* **14**, 293–321.

Zacharenkov, Yu.A., Zorev, N.N., Rupasov, A.A., Sklizkov, G.V. & Shikanov, A.S. (1983). Dynamics of plasma corona of spherical targets irradiated by a laser. In *Proc. P. N. Lebedev Phys. Inst.*, (Basov, N.G., Ed.) Vol. 133, pp. 146–188. Moscow: Nauka, in Russian.

Ziegler, J.F., Biersack, J.P. & Littmark, U. (1995). *The Stopping and Ranges of Ions in Solids*. New York: Pergamon Press.